THESIS

SEQUENTIAL EXPOSURE TO MANGANESE AND ENCEPHALITIC VIRAL INFECTION CAUSES A PARKINSONIAN PHENOTYPE LIKELY MEDIATED BY ASTROGLIOSIS

Submitted by

Lucas Hampton

Graduate Degree Program in Cell and Molecular Biology

In partial fulfillment of the requirements

For the Degree of Master of Science

Colorado State University

Fort Collins, Colorado

Spring 2021

Master's Committee:

Advisor: Carol Wilusz

Gerrit Bouma

Jozsef Vigh

ABSTRACT

SEQUENTIAL EXPOSURE TO MANGANESE AND ENCEPHALITIC VIRAL INFECTION CAUSES A PARKINSONIAN PHENOTYPE LIKELY MEDIATED BY ASTROGLIOSIS

Developmental exposure to environmental toxins increases neuronal susceptibility to injury from subsequent viral challenges. Neurodegenerative diseases such as Parkinson's Disease (PD) present with a neuroinflammatory component often linked to environmental risk factors—including toxic metals, chemicals, physical injury, and viral infection. While many of these risk factors are sufficient to cause a Parkinsonian disease state, none have been shown to be necessary, suggesting an underlying shared mechanism. Furthermore, for any individual risk factor, there is high variability regarding development and severity of the disease. One way to address these issues employs multiple risk factors to model the disease more accurately, although it is unclear how or why multiple unrelated insults have a compounding effect. Neuroinflammation is a shared consequence of the known environmental risk factors. Increased susceptibility to one insult following a challenge with another environmental toxicant may therefore be mediated by neuroinflammatory signaling cascades, a process largely regulated by glial cells, primarily astrocytes. Reactive astrocytes produce neuroinflammatory cytokines, the expression of which is governed by the transcription factor complex NF-κB, and its regulatory kinase, IKK2. The current study uses a two-hit model of environmental neurodegeneration, juvenile exposure to manganese (Mn) followed by adult infection with western equine encephalitic virus (WEEV). We found that WEEV alone produced a significant PD effect, evident by immunohistological staining of pathogenic markers and behavioral analyses; and that

WEEV and Mn exposure partially enhanced this effect. These exposures were conducted in both wildtype mice and in astrocyte-specific knockout mice lacking nuclear factor Ikappa-B kinase subunit beta (IKK-KO), hypothesizing that innate immune inflammatory signaling in reactive astrocytes modulates neuroinflammation and neuronal injury following combined exposure to Mn and WEEV. In multi-hit and single exposure treatment groups, IKK-KO mice displayed reduced viral replication and had decreased α-synuclein protein aggregation, astrogliosis and neuronal loss in multiple brain regions including the substantia nigra pars compacta, suggesting that astrocyte-mediated neuroinflammation may be one mechanism by which developmental toxin exposure can potentiate vulnerability to subsequent viral infections. Given the relevance of metal toxicity and viral infection to public health, these results provide insight into disease etiology and support further exploration of neuroinflammation as a mechanism of neurodegenerative pathologies.

TABLE OF CONTENTS

INTRODUCTION

Parkinson's Disease is a progressive neurodegenerative disease without a cure or long-term efficacious treatments. PD affects more than 10 million people worldwide [34], and disease prevalence is rapidly outpacing the overall age of the population. Rates of diagnosis dramatically increase after age 50 [19] and the disease is 1.5 times more prevalent in men than women [34]. The impacts of the disease at the social and personal level are tragic, but it also carries a significant economic burden. It is estimated that healthcare costs for PD in the United States are $53 billion per year (Parkinson's Foundation), and are expected to rise to $79 billion by 2037 [53].

While the impact of the disease is variable, common symptoms include bradykinesia, resting tremors, impacted bowel movements, and hyposomnia [20]. Symptoms of PD worsen as the disease progresses and can eventually lead to death. While the disease lacks any cure, several treatments delay the progression. The most effective treatment is levodopa, a precursor to dopamine. Developed in the 1960s, levodopa addresses the symptoms caused by deteriorated dopamine neurons by suppling the brain with a dopamine precursor, as dopamine itself cannot cross the blood brain barrier [54]; treatment options based on similar principles, such as inhibitors of monoamine oxidase B (MAOB)—the enzyme responsible for degrading dopamine, have also been developed. However patients treated with these drugs require frequent increases in dosage over the course of the treatment, which can be effective only up to about ten years, at which point the frequency and dosage begin to cause severe adverse effects such as levodopa-induced dyskinesia [54]. The dearth of treatment options is in large part due to a lack of understanding of the fundamental mechanisms of the disease.

The molecular basis of the disease is not well understood but is characterized by several well-defined pathological hallmarks—including loss of dopaminergic neurons in the substantia nigra pars compacta, aggregation of misfolded α-synuclein protein forming Lewy bodies, and neuroinflammation [27]. It is unclear whether these hallmarks have a causal relationship among each other or the disease itself. While neuronal loss in PD occurs predominantly in the substantial nigra, the disease affects the circuitry of the entire basal ganglia, a region critical for motor behavior [51]. A potential mechanism of the disease is the misfolding of α-synuclein. The insoluble protein aggregate, or the soluble oligomeric form, is thought to have a neurotoxic effect [52], leading to selective cell death of dopaminergic neurons in the substantia nigra [49], and subsequent neuroinflammation surrounding the damaged tissue. Researchers pursuing the α-synuclein hypothesis have proposed that the disease is prion like, as treatment with pathogenic α-synuclein protofibrils is sufficient to induce misfolding and aggregation of the native protein [50]. While the α-synuclein hypothesis has provided the field with invaluable insight into the disease, it has nonetheless failed to explain why neuronal loss is exclusive to motor cells in the substantia nigra, or culminate in disease treatments. A competing hypothesis turns the model on its head, suggesting that neuroinflammation is the primary cause and that protein aggregation is a downstream effect. Neuroinflammation can trigger neuronal death by proapoptotic cytokine signaling (e.g. TNF- α) or by cytokine induced oxidative stress [60, 61]. While the mechanisms by which inflammation causes cell death are not mutually exclusive, a number of neuroinflammatory PD models have focused on oxidative stress pathways as many of the PD genetic risk factors are implicated in redox signaling [29, 30, 44]. The neuroimmune hypothesis holds an advantage over competing PD hypotheses in explaining the regional specificity of

neurodegeneration; in fact many of the environmental risk factors associated with PD have been shown to have selective effects on PD-relevant brain regions.

While the central nervous system is largely considered to be immune privileged—protected from environmental insults by the blood-brain barrier—exposure to toxins, pollutants, and bacterial and viral infection have all been linked to PD [8, 33]. A prominent hypothesis that links environmental exposures to neurodegenerative diseases and models the stages of disease progression, Braak staging [4, 5], proposes that the central nervous system (CNS) is vulnerable to environmental exposures through both the olfactory bulb and enteric regions, finding that Lewy body lesions "initially occur in the dorsal motor nucleus of the glossopharyngeal and vagal nerves and anterior olfactory nucleus" [5]. Studies have supported this route of exposure, with one demonstrating that pathological alpha-synuclein travels from the gut to the brain through the vagus nerve [21].

One environmental risk factor associated with PD is viral exposure. Post-mortem examinations following the Spanish flu pandemic of 1918 [18] found "degenerative changes in the nerve cells…especially in the cells of the motor nuclei…" [47]—findings that are consistent with modern pathological observations of PD tissue. Other viruses that can cause Parkinsonian symptoms include western equine encephalitic virus (WEEV), Japanese encephalitis B (JEBV), and severe acute respiratory syndrome-coronavirus-2 (SARS-CoV-2)—among many others [55, 68]. While these viruses can cause motor neuron loss and behavioral phenotypes similar to PD patients, only WEEV has been reported to cause Lewy body formation [1, 55]. Neurological effects of WEEV include seizures, motor impairments, loss of taste, and intellectual disability [56]; the molecular effects of the disease are still poorly understood, but like other encephalitic infections, neuroinflammation has been observed [57]. Several patients in Colorado experienced

"rapid onset of postencephalitic parkinsonian sequelae," and were subsequently treated with levodopa and recovered within twelve months [40]. These findings have since prompted researchers to use WEEV to model the disease in animals. A recent study examined the effect of WEEV on PD in a mouse model. The researchers infected mice with WEEV and allowed the mice to recover for eight weeks following infection. The researchers then examined the neuroinflammatory response elicited by WEEV and if these mice developed a Parkinsonian phenotype. They found that infection with WEEV in mice causes Parkinsonian motor impairments, aggregates of proteinase-K resistant alpha-synuclein and increased astrocyte reactivity [1, 35].

Another environmental exposure that has been utilized to model PD is manganese. Manganese is a heavy metal used in industrial applications and has been shown to be a risk factor in many neurological disorders [3, 23]; a Parkinsonian phenotype associated with toxic manganese exposure is termed manganism. Manganese causes cytotoxicity by producing reactive oxygen species that disrupt mitochondrial function, eventually triggering apoptotic and necrotic signaling cascades [58]. Manganism can be caused by inhalation or ingestion of manganese, and is most prominent among individuals working in industrial settings—including mining, welding, and fossil fuel combustion [59]. Heavy metal toxicity has been linked to many types of neurodegeneration, although manganese is specifically linked to PD. This relationship, while not fully understood, may be because manganese accumulates in the basal ganglia, and thus may have a selective neurotoxic effect on neurons involved in motor circuitry.

Parkinson's disease is also linked to several genetic risk factors, the most notable of which are mutations in the E3 ubiquitin ligase PARKIN [29], the mitochondrial kinase PINK1 [30], and the LRRK2 kinase [44]. The LRRK2, leucine-rich repeat kinase 2, mutation is a

significant predictor of familial PD [64], and it is particularly relevant to neuroinflammatory models of the disease as it regulates autophagy induced by glial cells [63]. The most prominent pathogenic LRRK2 mutation occurs in its kinase domain, which leads to an increase in enzymatic activity; this increased activity disrupts a wide range of signaling cascades, including the mitogen-activated kinase pathway, Wnt signaling, and mitochondrial uncoupling [65]. A substantial component of LRRK2 dysregulation is increased glial mediated neuroinflammation, and it is unclear if the mutation in itself is a unique contributor to PD pathogenesis or if it is an alternative means to the inflammatory ends caused by environmental risk factors.

A multi-hit model of the disease is a more physiologically relevant representation of the environmental exposures in one's life that may lead to onset of the disease [32, 43]. A lingering question within the field is why some individuals who are exposed to manganese, or WEEV, develop the disease, whereas others who experience the same exposures do not? Development of Parkinson's disease may be attributed to an accumulation of exposures throughout one's life [6]. A biological process such as immune memory is a possible mechanism underlying such a compounding effect; and although this process has been historically attributed to the adaptive immune response, recent studies have demonstrated innate immune memory within glial cells of the nervous system[12, 45]. As the primary immune cells of the brain, and the central drivers of neuroinflammation, glial cells are an ideal target for investigating the links between Parkinson's Disease and sequential exposures to environmental risk factors.

Neuroinflammation is regulated by glial cells of the CNS, most notably astrocytes and microglia. Glial cells have been historically understood as simply regulators of CNS homeostasis, playing important roles in neurotransmitter recycling, modulating the extracellular milieu, and enhancing synaptic function [66]. Within the past several decades, our understanding

of glia has risen exponentially. Glial cells play vital roles in all the aforementioned processes, as well as CNS development, tissue repair, and neuroinflammation. Their function in modulating neuroinflammation is associated with many disease states including PD [67]. Inflammation induced by glial cells is caused by the release of cytokine signaling molecules, a majority of which are regulated by the transcription factor complex NF-κB [13]. Modulating NF-κB activity of glial cells has thus become a useful model in elucidating how risk factors that have a neuroinflammatory component contribute to diseases of the nervous system, this has become particularly relevant for environmental risk factors.

The two PD risk factors, WEEV and manganese, have been shown to cause severe neuroinflammation [35, 39]. This study uses both manganese and WEEV exposure to model the progression of PD while investigating the contribution of neuroinflammation through genetic manipulation of glial cells. These exposures were conducted in both wildtype mice and in astrocyte-specific knockout mice lacking nuclear factor Ikappa-B kinase subunit beta knockout (IKK2-KO). IKK2 regulates NF-κB nuclear translocation by phosphorylating the NF-κB inhibitor IκB— which is then degraded by ubiquitination (Fig. 1). Therefore, knocking out IKK results in constitutive inhibition of NF-κB and the inflammatory genes it regulates. Astrocyte specific KO mice are ideal for interrogating the neuroimmune response and isolating the contribution of glial cells to particular phenotypes. NF-κB in neurons is involved in a variety of cellular functions—including development and synaptic homeostasis; conversely, NF-κB in glial cells is highly expressed only during reactive states, and is primarily implicated in inflammation and disease [13]. Furthermore, while NF-κB signaling in astrocytes and microglia are both involved in neuroinflammation, microglia are typically the first responders nervous system injury—often secreting factors that recruit and activate astrocytes [2]. Astrocyte inflammatory

signaling being downstream of other glial cells allows for a more precise interrogation of the role of glial cells in neuronal injury. We hypothesize that innate immune inflammatory signaling in reactive astrocytes modulates neuroinflammation and neuronal injury following combined exposure to $MnCl_2$ and WEEV. At the study endpoint, eight weeks post-infection, mice were analyzed for WEEV replication, dopaminergic neuronal loss, alpha-synuclein aggregation, glial reactivity, and motor impairments.

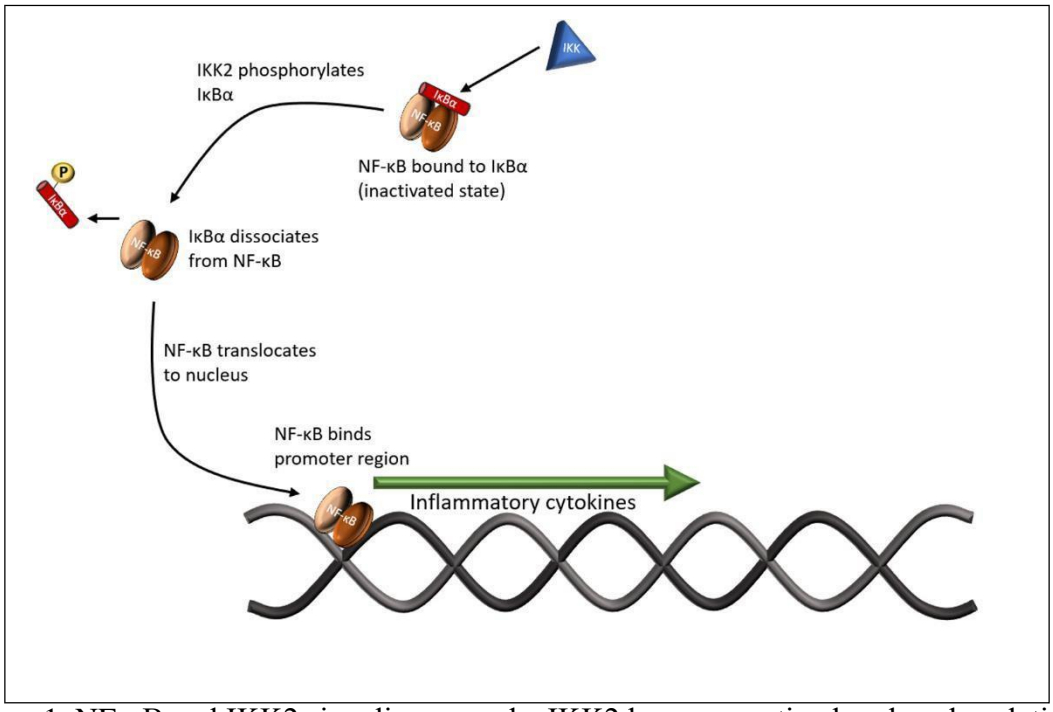

Figure 1. NF-κB and IKK2 signaling cascade. IKK2 becomes active by phosphorylation. In its active state, IKK2 phosphorylates IκBα. Phosphorylation of IκBα leads to its ubiquitination and degradation. The nuclear localization signal of the heterodimer, NF-κB, becomes exposed upon IKβ dissociation, and then translocates to the nucleus to trigger transcription of pro-inflammatory cytokines.

RESULTS

WEEV viral replication in the CNS is enhanced by juvenile exposure to manganese

A previous study [1] demonstrated that an intranasal inoculation of WEEV in wild-type mice propagated through olfactory bulbs, entorhinal cortex, hippocampus, ventral tegmental area (VTA) and substantia nigra (SN). We hypothesized that an inflammatory insult during juvenile stages of mouse development would potentiate a second inflammatory insult during the adult stages of life; specifically, we predict that the WEEV infection will be more severe in mice that are pretreated with $MnCl_2$. To test this hypothesis, juvenile mice were given drinking water supplemented with $MnCl_2$ (50mg/kg) for thirty days at a dose that has been shown to be subthreshold for primary toxic effects [31]. Mice were then aged into adulthood for another thirty days—and at which point were given an intranasal inoculation of WEEV. WEEV has been shown to be lethal in mice after four days [35], and therefore were given passive immunotherapy using rabbit antiserum against WEEV concurrent with infection, inoculation and dosing protocols were adapted from Bantle et al. 2019. Eight weeks after the cessation of $MnCl_2$ treatment, mice were intranasally inoculated with a dsRed-WEEV recombinant virus at a concentration of 1×10^4 PFU/ml (Fig. 2A). Mice were sacrificed 72 hours post-infection and viral replication was visualized by confocal microscopy. This timepoint was chosen based on prior findings that virus begins to clear from the brain as early as 72hr following infection. Infection was quantified by demarcating specific regions using the Allen Brain Atlas (Allen Mouse Brain Atlas 2004) and counting dsRed positive cells using Olympus Cellsens software. For each biological replicate (n=6), two technical replicate 10X montage images were acquired, and cell counts were averaged. Unpaired t-tests were performed using GraphPad Prism v9.0 comparing

cell counts within each region across treatment groups. The substantia nigra and hippocampus was quantified due to their relevance to Parkinson's disease [48] as well as their previous implication in WEEV viral infection [1].

Consistent with previous findings, regions of the brain infected with WEEV include entorhinal cortex, hippocampus, VTA, and SN (Fig. 2B). As expected, the $MnCl_2$ treatment group displayed an increase of dsRed positive cells (Fig 2C) in both the substantia nigra ($P<0001$) and the hippocampus ($P<0.001$). Further, in the $MnCl_2$ treatment group, viral presence was also detected in brain regions adjacent to those previously noted; for example, in the Mn/WEEV condition, viral infection was not only detected in the SN and VTA, but also in the mamillary bodies ventral to the VTA. The same is true for cortical regions surrounding the entorhinal cortex. These results demonstrate successful infection of mice with dsRed-WEEV and replication of prior findings that used a similar treatment regimen [1, 35]. Furthermore, these data suggest that treatment with $MnCl_2$ during the juvenile period does indeed potentiate the severity of WEEV infection in adulthood.

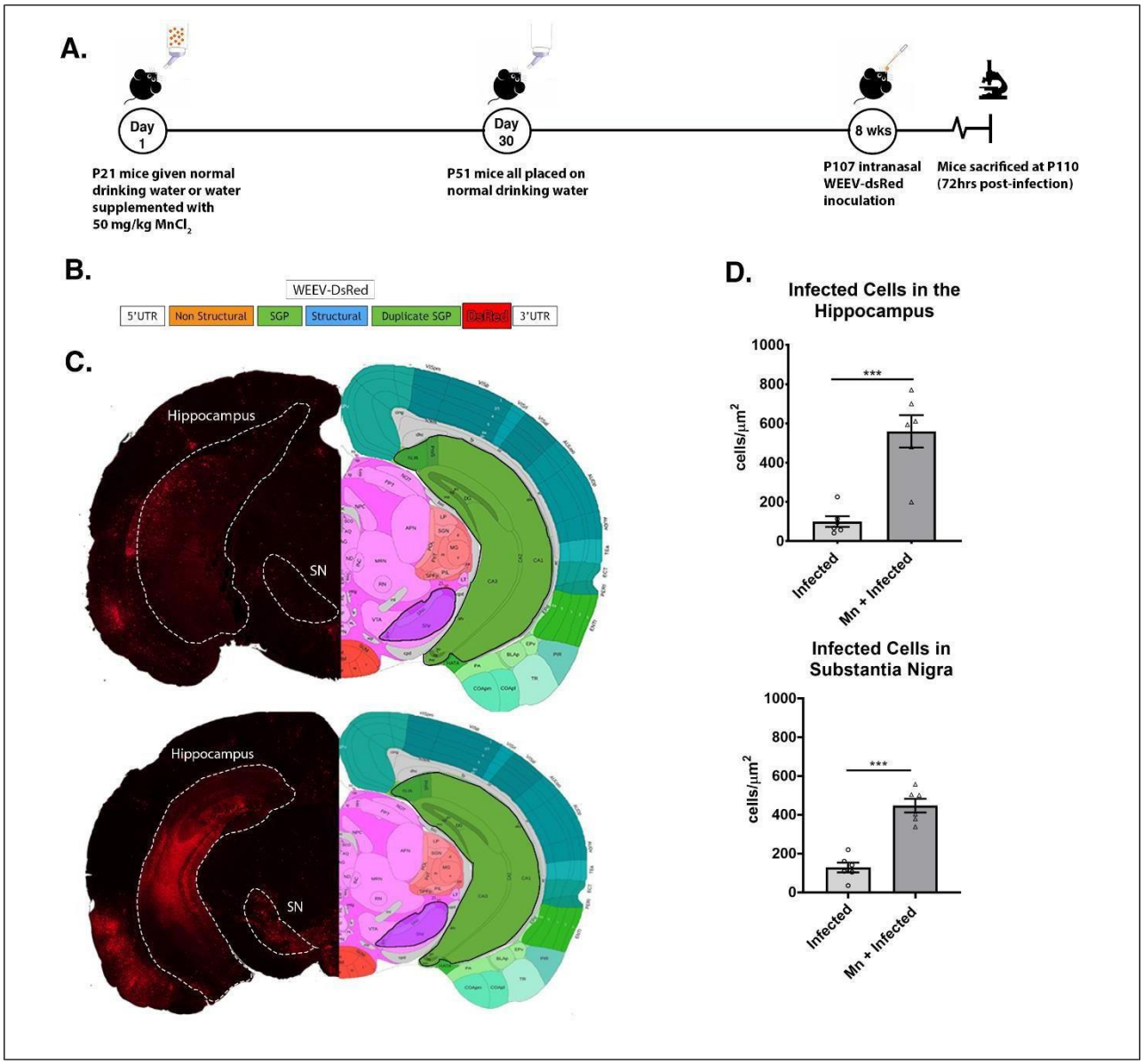

Figure 2. WEEV viral spread in the CNS is enhanced by juvenile exposure to manganese. Experimental paradigm is described in (A), and viral constructs are shown in (B); briefly, juvenile mice received either standard drinking water or water supplemented with 50mg/kg $MnCl_2$ for 30 days. All mice received standard drinking water for 30 days prior to inoculation with WEEV-dsRed or a sham vehicle inoculation. Mice were sacrificed 72hr post infection and examined for ds-Red expressing cells. (C) dsRed positive cells in coronal sections of mice receiving WEEV alone (above) or mice receiving $MnCl_2$ and WEEV (below). Allen mouse brain atlas overlayed on right hemisphere for orientation, specific regions quantified (substantia nigra and hippocampus) are highlighted in both hemispheres. (D) dsRed positive cells in each region across treatment groups. Total cell counts were divided by the area of each region; each data point is an average of two technical replicates for each biological replicate (n=6). SN = substantia nigra. *** = $p<0.001$.

A key inflammatory regulator, NF-κB, affects viral infection

Given the role of astrocytes in modulating the neuroimmune response [36], and the role of NF-κB in stimulating A1 astrocyte reactivity [24], we predict that knocking out this key inflammatory regulator in astrocytes will reduce replication of WEEV in both the $MnCl_2$ pretreatment and the WEEV alone groups. To gain insight into the role of glial-mediated neuroinflammation during WEEV infection, we also performed a pilot study in which we monitored WEEV replication at 72hr post-infection in astrocyte specific IKK2 KO transgenic mice using a WEEV-luciferase (WEEV-luc) recombinant virus. The WEEV-luc construct has been previously validated [1] and allows for live tracking of the virus during the course of the experiment.

Wild-type and transgenic animals were inoculated with WEEV-luc or sham inoculated eight weeks after cessation of $MnCl_2$ treatment (Fig. 3A). Seventy-two hours after inoculation mice were anesthetized, given a subcutaneous injection of luciferin at 150mg/kg, and imaged using the IVIS 200 bioluminescence imaging system. Background light emission was estimated from uninfected wild-type mice and subtracted from signal in WEEV infected mice.

Contrary to previous observations, wild-type mice that received $MnCl_2$ did not show a significant increase in reporter activity over mice that received WEEV alone ($p=0.08$; Fig. 3D); moreover, no effect was not observed when making the same comparison within the KO treatment group ($p=0.12$). Also contrary to our expectations, knockout of NF-κB signaling appeared to have no effect on viral replication, for no differences were detected between wild-type and KO mice. A power analysis of the experiment revealed the test is underpowered (power = 0.46) to detect differences between the conditions, and that a sample size of five per group would increase power to 0.80.

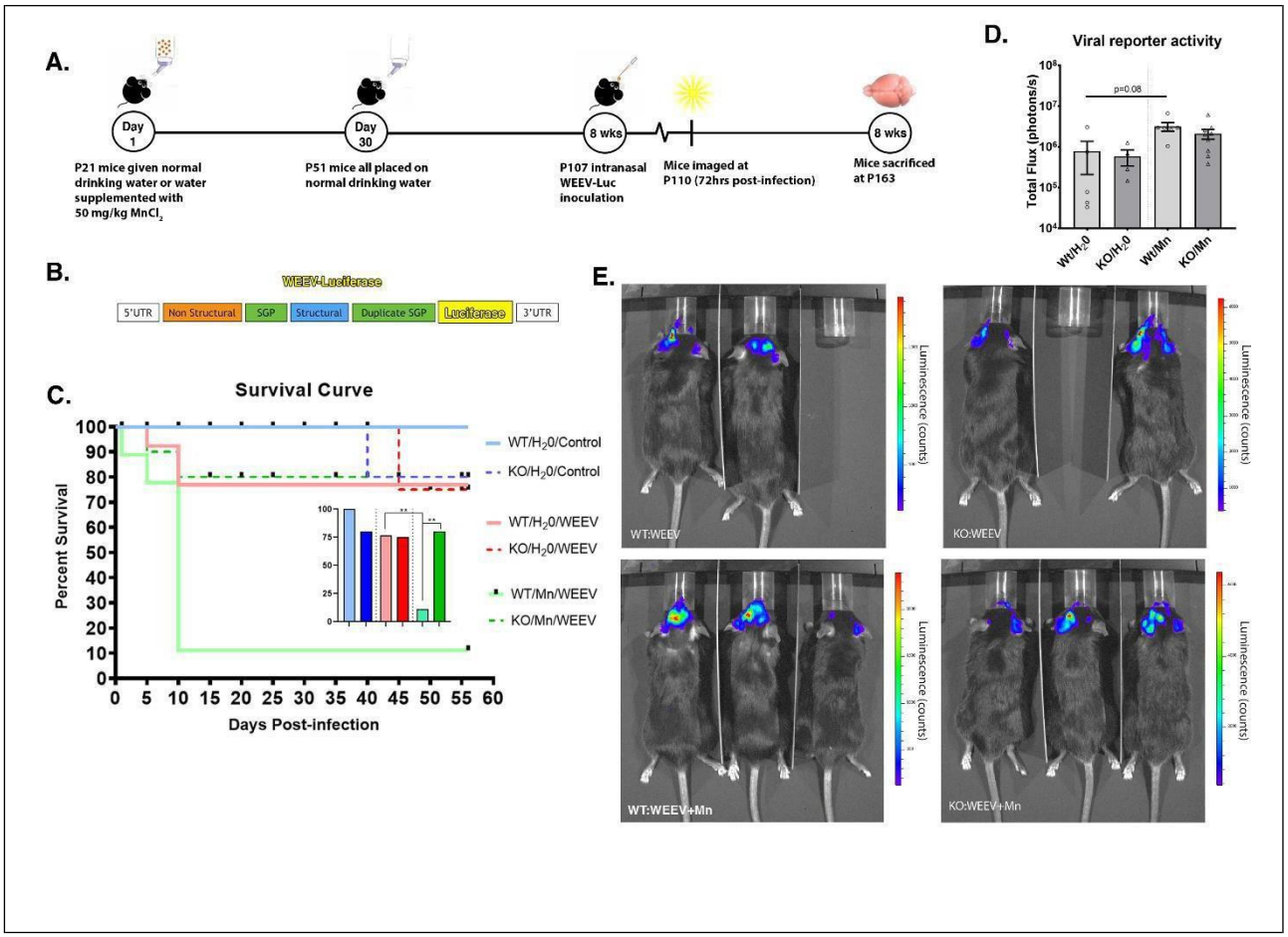

Figure 3. Knockout of key inflammatory regulator effects viral infection. Experimental strategy described in (A), and viral constructs are shown in (B). Bioluminescence of WEEV-luc mice is plotted in (D) as total flux (photons/s); no outliers were detected using ROUT detection in Graphpad Prism. Representative images of mice anesthetized with isoflurane using the XGI-8 anesthesia system (Caliper Life Sciences, Waltham, MA USA) and imaged using the IVIS 200 imaging system is shown in (E). Light emission is pseudo colored to represent counts of photons detected by CCD camera and overlayed onto mice in standard light conditions. Survival of mice throughout the course of the study is plotted in (C), Gehan-Breslow-Wilcoxon tests were used to determine differences between curves. n=6. * = $p<0.05$, ** = $p<0.01$, *** = $p<0.001$.

Reactive astrocytes in the CNS after viral infection

Inflammation in the nervous system is modulated by glia cells, primarily astrocytes and microglia [7, 9, 14]. In a reactive, or inflammatory, state, astrocytes upregulate expression of the intermediate filament GFAP [41]; this upregulation likely underlies concomitant morphological

changes that further characterize the reactive state of astrocytes [46]. Parkinsonian pathology instigated by sequential neuroinflammatory insults would likely be accompanied by an increase in the reactive astrocytosis in regions associated with PD. In our current model, it is expected that mice exposed to $MnCl_2$ prior to WEEV infection will display increased astrocyte reactivity compared to mice receiving WEEV alone. Furthermore, it is expected that knocking out NF-κB in astrocytes will result in less reactivity across all treatment groups.

Astrocyte reactivity was assessed by GFAP immunofluorescence in whole brain sections. Mice were perfused and selected tissue were fixed at P163, at eight weeks post-infection (n=4/treatment group). Tissue was dissected and embedded in paraffin for subsequent sectioning and staining. Coronal sections were stained with DAPI and monoclonal GFAP antibodies (see Methods) and imaged using an Olympus BX63 confocal microscope. GFAP positive cells were counted using Olympus Cellsens software in manually defined regions of interest.

An analysis of the survival curves (Fig. 3C) does reveal an effect of the dual-hit compared to WEEV alone in wild-type mice, although it is not clear if these differences are associated with increased astrocyte activity. The survival curve of the knockout dual hit group was not statistically different from all other treatment groups, suggesting that the dual-hit effect is mediated by NF-κB signaling in astrocytes.

WEEV infection alone displayed significantly higher GFAP expression compared to the control group in the SN ($p=0.03$) and cortex ($p=0.04$) (Fig. 4); however, no differences were detected within the hippocampus. Power analysis for tests within the SN and hippocampus revealed that this test was slightly underpowered (power = 0.43), and that increasing the sample size by one for each group would give more confidence in the differences observed. Mean differences in the hippocampus were by comparison much smaller, and thus would require a

dramatic increase in sample size to detect differences. Whether or not differences were observed in the dual-hit treatment group is unknown, for a vast majority of mice within the wt/Mn/WEEV treatment group did not survive the full duration of the treatment regimen (Fig. 3C). While we were not able to compare GFAP expression in KO/Mn/WEEV to wt/Mn/WEEV, comparisons between wt/H_2O/WEEV and KO/H_2O/WEEV were used to shed light on the relevance of astrocyte NF-κB signaling during WEEV infection. While mean GFAP expression levels trend lower in the KO group, statistical differences between the two groups were not detected in any of the regions examined. These results show that WEEV infection is sufficient to elicit a reactive phenotype in astrocytes in several brain regions, and that mice in the KO group are not differentially affected by WEEV infection.

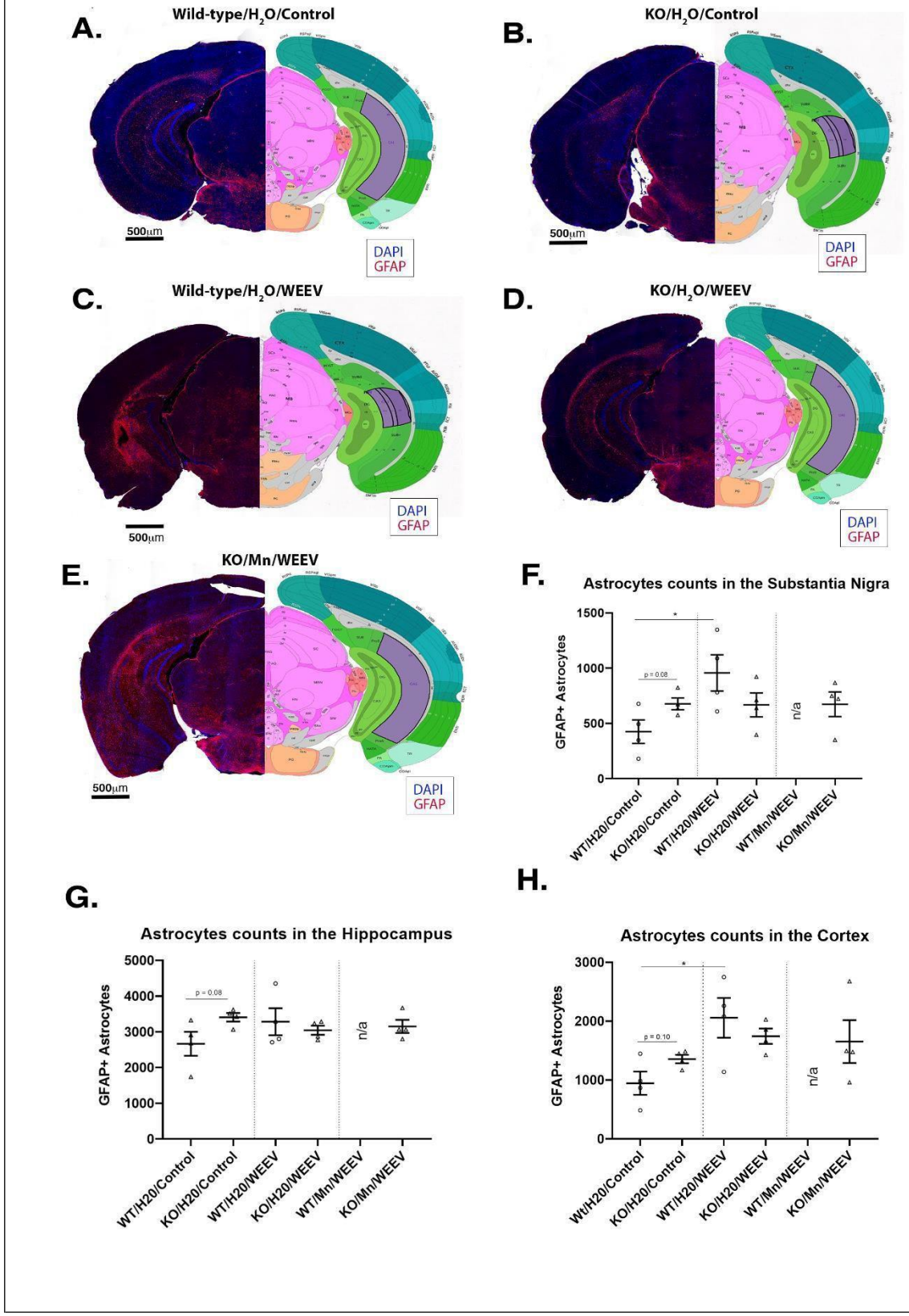
A.
Wild-type/H2O/Control
500µm
DAPI
GFAP
B.
KO/H2O/Control
500µm
DAPI
GFAP
C.
Wild-type/H2O/WEEV
500µm
DAPI
GFAP
D.
KO/H2O/WEEV
DAPI
GFAP
E.
KO/Mn/WEEV
500µm
DAPI
GFAP
F.
Astrocytes counts in the Substantia Nigra
GFAP+ Astrocytes
1500
1000
500
0
*
p = 0.08
n/a
WT/H20/Control
KO/H20/Control
WT/H20/WEEV
KO/H20/WEEV
WT/Mn/WEEV
KO/Mn/WEEV
G.
Astrocytes counts in the Hippocampus
GFAP+ Astrocytes
5000
4000
3000
2000
1000
0
p = 0.08
n/a
WT/H20/Control
KO/H20/Control
WT/H20/WEEV
KO/H20/WEEV
WT/Mn/WEEV
KO/Mn/WEEV
H.
Astrocytes counts in the Cortex
GFAP+ Astrocytes
3000
2000
1000
0
*
p = 0.10
n/a
Wt/H20/Control
KO/H20/Control
WT/H20/WEEV
KO/H20/WEEV
WT/Mn/WEEV
KO/Mn/WEEV

Figure 4. Reactive astrocytes in PD-relevant brain regions. Whole brain 10X montage images showing GFAP in red counterstained with DAPI (A-E); corresponding sections from the Allen Mouse Brain Atlas is overlayed onto right hemisphere. F – G showing quantification of astrocytes in relevant brain regions; all counts are of single hemisphere. * = $p<0.05$, ** = $p<0.01$, *** = $p<0.001$.

IKK2 KO rescues behavioral deficits in mice infected with WEEV

Behavioral hallmarks of Parkinson's Disease include motor deficits such as tremors, bradykinesia, and imbalance [10]. To assess these clinical features in our experimental model, a mouse trackway system was developed to monitor movement across an enclosed glass platform (Fig. 5A). Mice paw pads were recorded from an upward facing camera below the platform and gait analysis was performed using MATlab software. Data extrapolated includes paw support, run duration, step size, swing speed, and swing time. More details of this trackway system are described in Hammond et al. 2018.

A previous study has shown that WEEV infection causes motor deficits in mice; therefore, we expect that these findings will be replicated in our wild-type mice. Moreover, the increased severity of WEEV infection caused by $MnCl_2$ should exacerbate these effects. Wild-type mice were compared against IKK2 KO mice with the prediction that knocking out inflammatory signaling in astrocytes will ameliorate the motor effects associated with $MnCl_2$ and WEEV.

Behavioral gait analysis was performed immediately prior to sacrifice. Mice were placed in the trackway system in low light conditions during mouse subjective night. Mice moved across the 1-meter platform towards their home cage at the end of the platform. Light was projected above the mice and paw prints were recorded from below the platform. Swing speed was measured as the speed (cm/s) of the same mouse paw starting at the initiation of movement

from one step to the next. Swing time was recorded as the time (s) between initiating steps, and run duration was the time to reach their home cage once movement in the correct direction was initiated. No meaningful differences were detected in swing speed; however, run duration was significantly higher in wild-type WEEV infected mice compared to all other treatment groups. (Fig 5), with the KO/H_2O/WEEV and KO/Mn/WEEV being significantly lower. The two wt/Mn/WEEV mice that survived throughout the experimental regimen were not able to complete the trackway, and thus were not included in the analysis. No differences were observed in paw support for any group comparison (Fig. 5). These results indicate that WEEV infection causes Parkinsonian-like motor deficits in mice, and that these effects may be mediated by NF-κB signaling in astrocytes. All behavioral analyses with the exception of run duration were well powered to detect group differences. Increasing the sample size by one would have brought power levels to eighty percent in the run duration analysis.

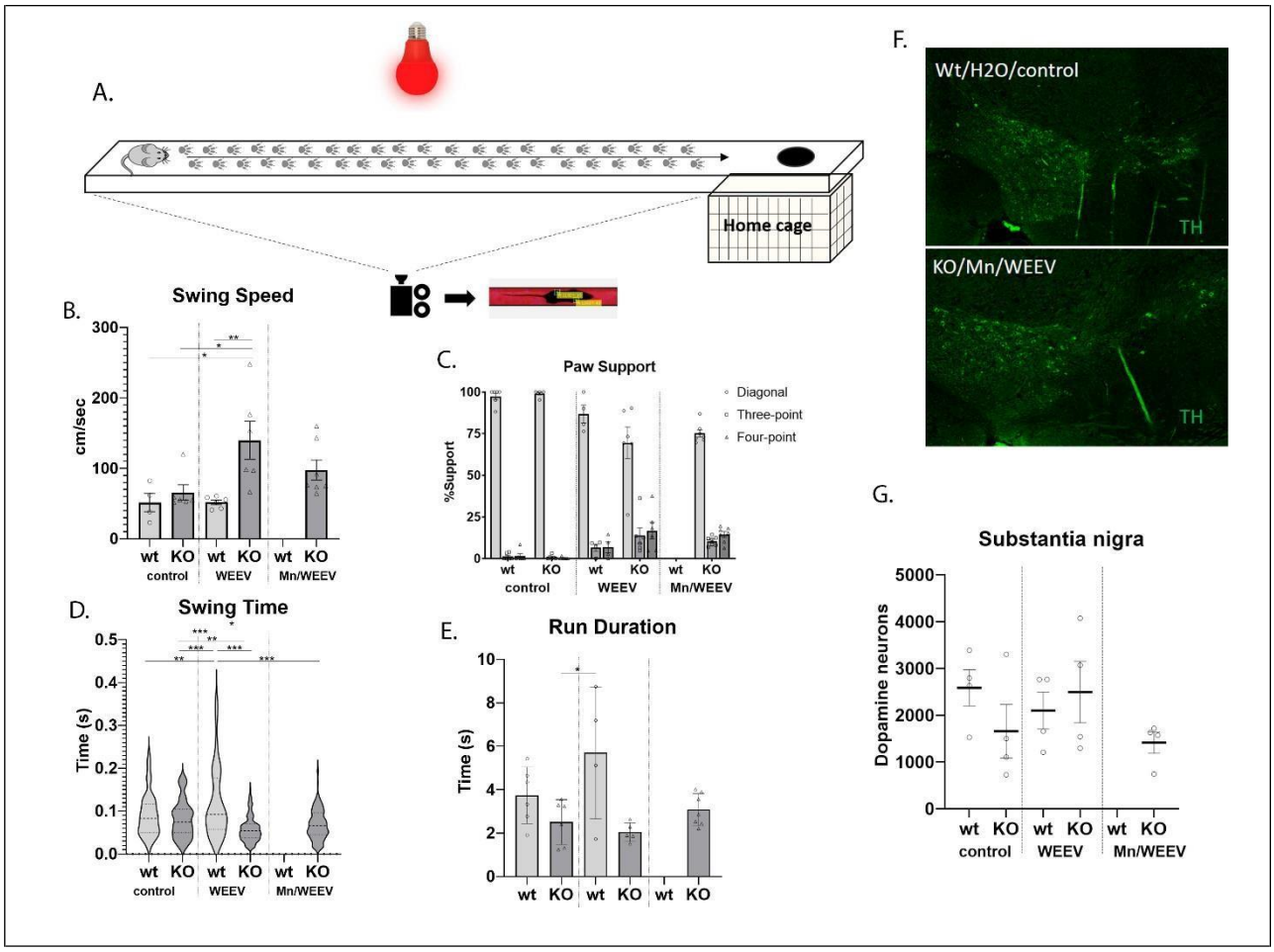

Figure 5. Behavioral deficits in mice infected with WEEV and dopaminergic neuron counts in the substantia nigra. Mice were placed in trackway shown in (A) and foot pads were tracked as mice moved towards their home cage. The time between paw swings (A), the duration until mice reached their home cage (C), and (D) the speed at which paws moved—once swing was initiated—was quantified using MATLAB software. Representative images of dopaminergic neuron staining in (F), and quantifications in (G). * = $p<0.05$, ** = $p<0.01$, *** = $p<0.001$.

Alpha-synuclein aggregation during WEEV infection in wild-type and IKK2 KO mice

A major clinical feature of Parkinson's Disease is the presence of alpha-synuclein aggregates in the brain. These aggregates are phosphorylated at the S129 residue and are resistant to digestion by proteinase K. Phosphorylated-alpha synuclein is being investigated as an early biomarker of PD [62], and thus demonstrating the presence of these aggregates is critical in establishing an animal model to study the disease [15].

Alpha-synuclein aggregation during WEEV infection was monitored by immunofluorescent staining of the P129 residue. Stained sections were evaluated blinded using a previously validated pathological scoring method [37]. Briefly, a the blinded researcher was asked to score the presence of aggregates in selective regions on a 1-5 scale (1 = no P129+ aggregates or cells, 2 = few/sparse aggregates with less than three cells, 3 = multiple aggregates with no more than 10 cells, 4 = dense aggregates with more than 10 P129+ cells, 5 = very dense aggregates with more than 20 cells).

WEEV infection in mice has been shown to induce aggregation of PK-resistant P129 alpha-synuclein [1]. This finding was replicated in all three regions (SN, hippocampus, cortex) examined in the current study (Fig. 6F-H, $p<0.001$). Moreover, the severity of these aggregates was found to be significantly reduced in the IKK2 KO mice compared to wild-type in all three regions; however, when comparing the KO/H2O/WEEV condition to the wild-type control, aggregate levels in the cortex ($p=0.001$) and hippocampus ($p<0.001$) were only partially rescued by the knock-out. KO/Mn/WEEV aggregates were significantly higher than KO/H_2O/WEEV in the SN ($p=0.02$), but not in cortex or hippocampus (Fig. 6). The effect of the knockout on the Mn/WEEV dual treatment in wild-type could not be evaluated due to survivability of mice in that condition. All p129 multiple comparison tests were well powered to detect differences.

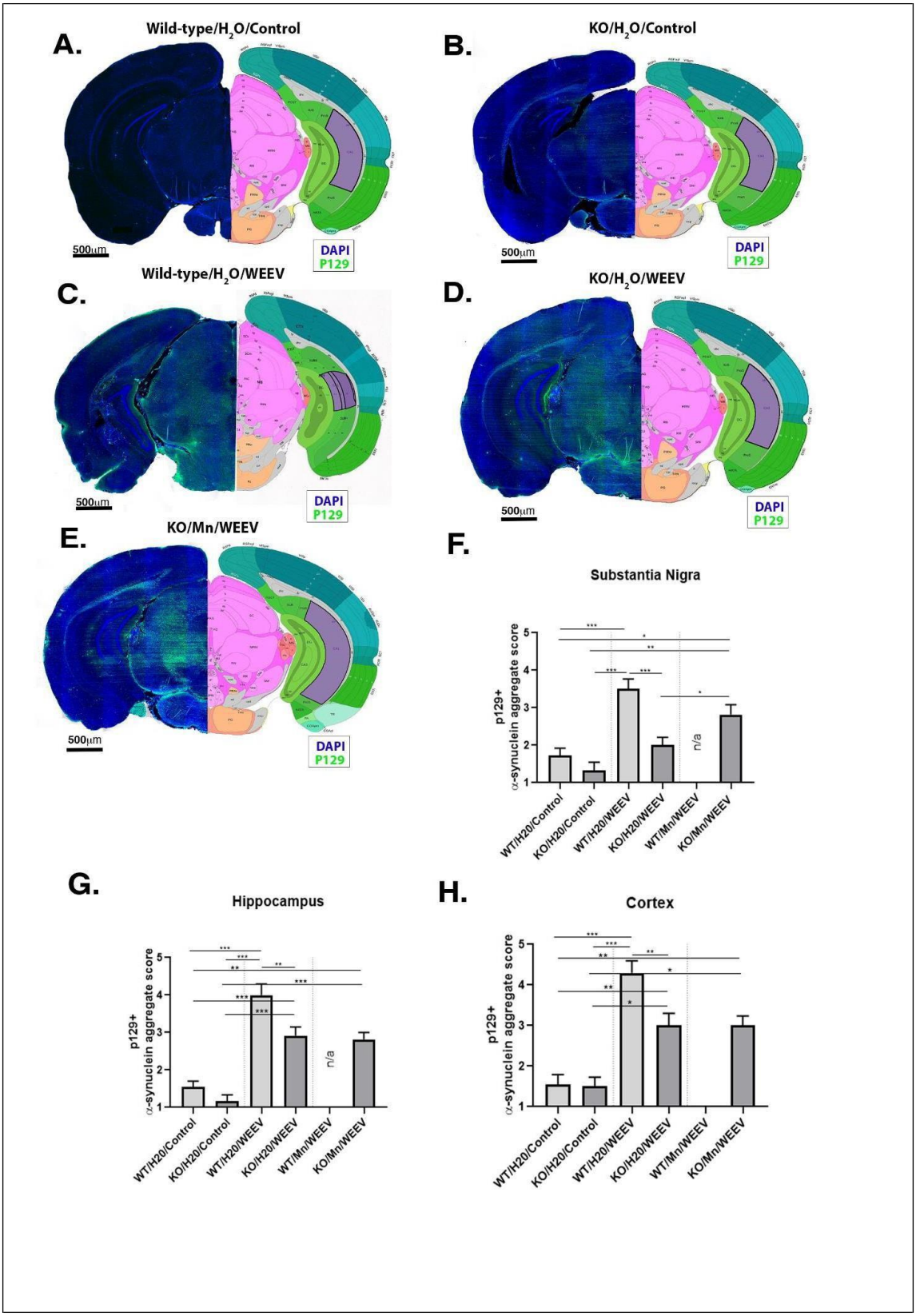
A.
Wild-type/H2O/Control
500μm
DAPI
P129
B.
KO/H2O/Control
500μm
DAPI
P129
C.
Wild-type/H2O/WEEV
500μm
DAPI
P129
D.
KO/H2O/WEEV
500μm
DAPI
P129
E.
KO/Mn/WEEV
500μm
DAPI
P129
F.
Substantia Nigra
α-synuclein aggregate score
p129+
n/a
WT/H20/Control
KO/H20/Control
WT/H20/WEEV
KO/H20/WEEV
WT/Mn/WEEV
KO/Mn/WEEV
G.
Hippocampus
α-synuclein aggregate score
p129+
n/a
WT/H20/Control
KO/H20/Control
WT/H20/WEEV
KO/H20/WEEV
WT/Mn/WEEV
KO/Mn/WEEV
H.
Cortex
α-synuclein aggregate score
p129+
WT/H20/Control
KO/H20/Control
WT/H20/WEEV
KO/H20/WEEV
WT/Mn/WEEV
KO/Mn/WEEV

Figure 6. Alpha synuclein aggregation during WEEV infection in wild-type and IKK2 KO mice. Alpha synuclein aggregation was assessed by whole brain immunofluorescent staining in wild-type and IKK2 KO mice (A-E). Aggregates were scored blinded on a scale of 1-5 and quantified in selective regions; the substantia nigra (F), hippocampus (G), and cortex (H). * = $p<0.05$, ** = $p<0.01$, *** = $p<0.001$.

Selective loss of dopaminergic neurons in the substantia nigra

A hallmark of Parkinsonian diseases is the loss of dopaminergic neurons in the substantia nigra, with the population of neurons in the substantia nigra *pars* reticulata being at the most risk. Loss of these neurons was evaluated by immunofluorescent staining in serial sections that spanned the nigral regions. Neurons were counted for positive fluorescence in regions of interest, and total neuronal counts were estimated based the width of the sections, the number of sections counted, and the distance between each section; volumetric counts were adapted from a previously described method [69]. No differences were detected between wt/control and wt/WEEV mice (representative section images in Fig. 5F). No mice in the wt/Mn/WEEV treatment group survived at the 8-week time point, so no comparisons were able to be made (Fig 5G). These tests were slightly underpowered, for the high variability in neuronal counts within animals and the relatively small mean differences between groups would require a sample size of sixteen animals per group to detect significant mean differences between conditions.

DISCUSSION

This study successfully demonstrates the validity of the multiple-hit model of Parkinson's disease, and while this model has been described in prior studies [32, 43], it is unique in that it captures multiple facets of disease pathology; namely, neuroinflammation, alpha-synuclein aggregates, and motor deficits. While it has been demonstrated that WEEV can produce a parkinsonian phenotype, it was unknown of the effect can be enhanced by a second environmental insult—an accurate representation of PD etiology. Adding the novelty and physiological relevance of this model, this study demonstrates that this multi-hit potentiation of PD is partially mediated by neuroinflammatory signaling in astrocytes. However, the significant loss of animals in the wt/Mn/WEEV experimental group leaves the interpretation of such effects ambiguous. Furthermore, while the genetic knockout of IKK2 was found to be protective in regard to viral spread, and astrogliosis, and motor impairments, the knockout did not fully protect against the development of alpha-synuclein aggregates or the loss of dopaminergic neurons—in fact showing a baseline effect of neuronal loss. While there is a strong body of literature suggesting that genetic knockout of IKK2 can have a protective effect in models of neurodegeneration [22, 26, 38], it has also been suggested that timing of NF-κB activation/inactivation is critical in modulating the progression and severity of disease states [11]. Future studies would benefit from inducible transgenic manipulation of NF-κB signaling.

Another future direction to consider is the interaction of these environmental risk factors and genetic risk factors. To further elucidate the contribution of neuroinflammation to disease pathogenesis, it is necessary to manipulation inflammatory signaling in the CNS using transgenic models that contain PG genetic risk factors. It would be interesting to examine if a PD phenotype

observed in genetic models is rescued by dampening inflammatory signaling, and if this effect can be reversed by including an inflammatory environmental risk factor. Lastly, this study used the IKK2 KO as a means of knocking out NF-κB driven inflammation in glial cells, but we did not consider other targets of IKK2. It has been shown that LRRK2 is a target of IKK2, and that phosphorylation of LRRK2 increases its own kinase activity—which leads to a PD disease state. Perhaps IKK2 is relevant to PD over and above its function in IκBα phosphorylation.

Perhaps the most striking observation within the current study is the dramatic loss of animals in the wild-type Mn/WEEV condition. While the loss prevented further analysis from determining whether the increased mortality was paired with increased neuronal inflammation, selective neuronal loss, or presence of insoluble protein aggregates, it is clear these mice were protected by the modulation of NF-κB signaling in astrocytes, possibly though similar mechanisms by which the WEEV treatment group was protected against the aforementioned pathological hallmarks. An alternative explanation that is unrelated to the pathophysiology of PD is that inhibiting NF-κB signaling increases the efficacy of the adjunct immunotherapy administered during WEEV infection. As previously discussed, WEEV infection is highly lethal in wild-type mice [35] without immunotherapy. Astrocyte-derived cytokines—both pro and anti-inflammatory—play an important role in blood-brain barrier integrity, CNS macrophage reactivity, and recruitment of peripheral macrophages from the bloodstream [7, 28]. Perhaps subtle changes in NF-κB-dependent cytokine expression in astrocytes have global impacts on macrophage activity in the central and peripheral systems.

Despite the lack of data in the wild-type Mn/WEEV group, this study sheds light on the role of astrocyte-derived neuroinflammation in the development of Parkinson's disease. We have shown that the combination of manganese and WEEV results in increased severity of subsequent

neuroinflammatory responses that persists eight weeks after infection. Furthermore, either in conjunction with, or as a result of this neuroinflammatory model, mice developed aggregated of alpha-synuclein in the substantia nigra, hippocampus, and several cortical regions and displayed motor impairments similar to those of Parkinson's disease. In support of the hypothesis that these parkinsonian features are caused by glial-derived neuroinflammation, knocking out a key regulator of neuroinflammation in astrocytes ameliorated many of these effects. Together, these data lend further support to glial-derived neuroinflammation as a causative rather than symptomatic feature of the molecular basis of Parkinson's disease.

METHODS

DsRed and firefly Luciferase recombinant WEEV constructs

The subgenomic promoter (SGP) sequence (nucleotides 7341–7500 of viral genome) of WEEV McMillan strain was duplicated to express DsRed and Firefly luciferase. Plasmids were purified using the QIAprep Spin MiniPrep Kit (Qiagen, Valencia, CA USA) and subsequently transcribed using T7 RNA polymerase (MAXIscript™ kit, Life Technologies, Grand Island, NY USA). Recombinant plasmids were then transfected with 20 µL of total RNA using an ECM 630 electroporator (BTX Harvard Apparatus, Holliston, MA USA) in BHK-21cells (2×107 in 400 µL). After transfection, virus was collected and stored at −80°C before quantification of viral concentration with plaque assays.

Generation of astrocyte-specific knockout mice

Astrocyte specific knockout mice for IKK2 were generated as previously described [37]. Briefly, *hGfap-cre*$^{+/-}$ (Cat#: 004600; Jackson Laboratories) mice were backcrossed on a C57/BlJ6 background for twelve generations before crossbreeding with *Ikk2-loxP*$^{+/+}$mice. Four generations of crossbreeding were conducted to acquire *hGfap-cre*$^{+/-}$/*Ikk2-loxP*$^{+/+}$ (KO). Littermates lacking Cre recombinase (*hGfap-cre*$^{-/-}$/*Ikk2-loxP*$^{+/+}$) were used as genotype controls for the study.

Viral infections and manganese chloride treatment regimen in control and transgenic mice.

Procedures were approved by Colorado State University Institutional Animal Care and Use Committee (IACUC) and were conducted in compliance of National Institute of Health guidelines. Infected mice were housed in a biosafety level 3 (BSL-3) facility at the Infectious Disease Research Center on the campus of Colorado State University. C57BL/6 astrocyte-

specific knockout mice (*Gfap -Cre*$^{+/-}$ mice with *Ikk2-loxP*$^{+/+}$) and control mice (*Gfap -Cre*$^{-/-}$ mice with *Ikk2-loxP*$^{+/+}$) were housed on a 12 hr light/dark cycle in a temperature-controlled room (maintained at 22-24°C). At day P21, mice were administered $MnCl_2$ (50mg/kg/day) or normal drinking water by monitoring water intake and weight gain for 30 days. At P51 mice were placed back on regular drinking water and intranasally administered WEEV-DsRed, WEEV-Luc, or saline. Infections with recombinant WEEV were performed as previously described [9]. Mice were anesthetized with isoflurane (Minrad Inc, Bethlehem, PA USA) in an XGI-8 anesthesia system (Caliper Life Sciences, Waltham, MA USA) and imaged using an IVIS 200 (Caliper Life Sciences, Waltham, MA USA) bioluminescence imaging system. Lightly anesthetized mice were then administered 20 µL dropwise on the nostrils of either DsRed-WEEV or Luc-WEEV at a concentration of 1×10^4 PFU/ml. All mice infected with Luc-WEEV received a subcutaneous administration of luciferin at a dose of 150 mg/kg, 10-15 minutes prior to imaging on an IVIS imager. For background subtractions, uninfected mice were used as image controls. All mice were imaged on the same exposure time at 2 minutes, under standard settings for the IVIS 200 camera. Image analysis was performed on Living Image 3.0 software (Caliper Life Sciences, Waltham, MA USA). Total light emission from each mouse was determined by creating a region of interest (ROI) of standard size for each mouse and collecting light emission data. Infected mice and control mice received an anti-E1 therapy intraperitoneally at 12 and 48hrs post-infection.

Tissue preparation and sectioning

Ten-day and eight-week post-infection with Luc-WEEV, animals were terminally anesthetized with isoflurane and transcardially perfused. The brains were then extracted, fixed in 3% paraformaldehyde at 4°C and later processed for paraffin embedding and sectioning at 8 microns.

Immunofluorescent Staining and Imaging

Sections were paraffin embedded and mounted on glass slides and stored at room temperature away from light. Prior to staining, sections were deparaffinized using a Leica Bond RXM automated robotic staining system. Tissue was permeabilized using Bond Epitope Retrieval Solution for 30 minutes and incubated with primary antibody for one-hour (anti-tyrosine hydroxylase (TH; 1:500; Millipore AB152), anti-glial fibrillary acidic protein (GFAP; 1:500; DAKO Z0334), anti-serine phosphorylated 129 (p129; 1:100; WAKO pSYN#64). Antibodies were diluted according to manufacturer's recommendations in TBS and 0.01% TX-100. Sections were washed in antibody dilution buffer 3 time prior to secondary antibody incubation, which was performed at room temperature for 1 hour. Slides were then coverslipped using ProLong™ Gold Antifade Mountant with DAPI (ThermoFischer P36931) and stored at room temperature away from light until imaging. DsRed-WEEV tissue was prepared similarly without antibody incubation or nuclear counterstaining. Sections were imaged using a Hammatsu Flash4.0 digital CMOS camera, ProScan III stage controller (Prior, Rockland, MA USA) and CellSens Dimension software (version 1.12, Olympus, Center Valley, PA, USA).

Behavioral Analysis

Following previously established protocols, mice were acclimated to handling, and the gain analysis trackway two weeks before infections [16, 42]. Baseline measurements were taken one day before infections with WEEV. As previously described, multiple neurobehavioral parameters, including, run duration, swing speed, swing time, and paw support were measured using a real-time video gait analysis system [17]. All behavioral testing was performed on uninfected and infected mice on days 0 and 56. All parameter values were normalized by

subtracting from the baseline measurements obtained on day 0 to normalize across all time points and treatment groups.

Statistical Analysis

All statistical analyses were performed using GraphPrism (version 9.0.0, Graph Pad Software, San Diego, CA) and SigmaPlot (version 14.5, Systat Software, San Jose, CA). All data points were assessed for outliers using ROUT (α=1%), and outliers were excluded from analyses. Group comparisons were analyzed by one-way ANOVA and post-hoc pairwise Tukey tests. Significant was defined as $p<0.05$. Power analysis was performed using SigmaPlot. All reported error is presented as the standard error of the mean (SEM).

REFERENCES

[1] Bantle, C. M., Phillips, A. T., Smeyne, R. J., Rocha, S. M., Olson, K. E., & Tjalkens, R. B. (2019a). Infection with mosquito-borne alphavirus induces selective loss of dopaminergic neurons, neuroinflammation and widespread protein aggregation. *Npj Parkinson's Disease*, *5*(1), 20. https://doi.org/10.1038/s41531-019-0090-8

[2] Bernaus, A., Blanco, S., & Sevilla, A. (2020a). Glia Crosstalk in Neuroinflammatory Diseases. *Frontiers in Cellular Neuroscience*, *14*, 209. https://doi.org/10.3389/fncel.2020.00209

[3] Bowman, A. B., Kwakye, G. F., Herrero Hernández, E., & Aschner, M. (2011). Role of manganese in neurodegenerative diseases. *Journal of Trace Elements in Medicine and Biology*, *25*(4), 191–203. https://doi.org/10.1016/j.jtemb.2011.08.144

[4] Braak, H., & Braak, E. (1991). Neuropathological stageing of Alzheimer-related changes. *Acta Neuropathologica*, *82*(4), 239–259. https://doi.org/10.1007/BF00308809

[5] Braak, Heiko, Tredici, K. D., Rüb, U., de Vos, R. A. I., Jansen Steur, E. N. H., & Braak, E. (2003). Staging of brain pathology related to sporadic Parkinson's disease. *Neurobiology of Aging*, *24*(2), 197–211. https://doi.org/10.1016/S0197-4580(02)00065-9

[6] Cabezudo, D., Baekelandt, V., & Lobbestael, E. (2020). Multiple-Hit Hypothesis in Parkinson's Disease: LRRK2 and Inflammation. *Frontiers in Neuroscience*, *14*, 376. https://doi.org/10.3389/fnins.2020.00376

[7] Carson, M. J., Cameron Thrash, J., & Walter, B. (2006). The cellular response in

neuroinflammation: The role of leukocytes, microglia and astrocytes in neuronal death and survival. *Clinical Neuroscience Research*, *6*(5), 237–245. https://doi.org/10.1016/j.cnr.2006.09.004

[8] Chen, H., & Ritz, B. (2018). The Search for Environmental Causes of Parkinson's Disease: Moving Forward. *Journal of Parkinson's Disease*, *8*(s1), S9–S17. https://doi.org/10.3233/JPD-181493

[9] Cherry, J. D., Olschowka, J. A., & O'Banion, M. (2014a). Neuroinflammation and M2 microglia: The good, the bad, and the inflamed. *Journal of Neuroinflammation*, *11*(1), 98. https://doi.org/10.1186/1742-2094-11-98

[10] Clarke, C. E. (2007). Parkinson's disease. *BMJ*, *335*(7617), 441–445. https://doi.org/10.1136/bmj.39289.437454.AD

[11] Dokalis, N., & Prinz, M. (2018). Astrocytic NF-κB brings the best and worst out of microglia. *The EMBO Journal*, *37*(16). https://doi.org/10.15252/embj.2018100130

[12] Domínguez-Andrés, J., & Netea, M. G. (2020). The specifics of innate immune memory. *Science*, *368*(6495), 1052–1053. https://doi.org/10.1126/science.abc2660

[13] Dresselhaus, E. C., & Meffert, M. K. (2019a). Cellular Specificity of NF-κB Function in the Nervous System. *Frontiers in Immunology*, *10*, 1043. https://doi.org/10.3389/fimmu.2019.01043

[14] Giovannoni, F., & Quintana, F. J. (2020). The Role of Astrocytes in CNS Inflammation. *Trends in Immunology*, *41*(9), 805–819. https://doi.org/10.1016/j.it.2020.07.007

[15] Gómez-Benito, M., Granado, N., García-Sanz, P., Michel, A., Dumoulin, M., & Moratalla, R. (2020a). Modeling Parkinson's Disease With the Alpha-Synuclein Protein. *Frontiers in Pharmacology*, *11*, 356.

https://doi.org/10.3389/fphar.2020.00356

[16] Gouveia, K., & Hurst, J. L. (2013). Reducing Mouse Anxiety during Handling: Effect of Experience with Handling Tunnels. *PLoS ONE*, *8*(6), e66401. https://doi.org/10.1371/journal.pone.0066401

[17] Hammond, S. L., Popichak, K. A., Li, X., Hunt, L. G., Richman, E. H., Damale, P. U., Chong, E., K. P., Backos, D. S., Safe, S., & Tjalkens, R. B. (2018). The Nurr1 Ligand,1,1-bis(3′-Indolyl)-1-(*p* -Chlorophenyl)Methane, Modulates Glial Reactivity and Is Neuroprotective in MPTP-Induced Parkinsonism. *Journal of Pharmacology and Experimental Therapeutics*, *365*(3), 636–651. https://doi.org/10.1124/jpet.117.246389

[18] Henry, J., Smeyne, R. J., Jang, H., Miller, B., & Okun, M. S. (2010). Parkinsonism and neurological manifestations of influenza throughout the 20th and 21st centuries. *Parkinsonism & Related Disorders*, *16*(9), 566–571. https://doi.org/10.1016/j.parkreldis.2010.06.012

[19] Hirsch, L., Jette, N., Frolkis, A., Steeves, T., & Pringsheim, T. (2016). The Incidence of Parkinson's Disease: A Systematic Review and Meta-Analysis. *Neuroepidemiology*, *46*(4), 292– 300. https://doi.org/10.1159/000445751

[20] Kuan, W.-L., & John van Geest (2018). Parkinson's Disease: Etiology, Neuropathology, and Pathogenesis. In John Van Geest Centre for Brain Repair, Department of Clinical Neurosciences, University of Cambridge, UK (2018). *Parkinson's Disease: Pathogenesis and Clinical Aspects* (pp. 3–26). Codon Publications. https://doi.org/10.15586/codonpublications.parkinsonsdisease.2018.ch1

[21] Kim, S., Kwon, S.-H., Kam, T.-I., Panicker, N., Karuppagounder, S. S., Lee, S., Lee, J. H., Kim,W. R., Kook, M., Foss, C. A., Shen, C., Lee, H., Kulkarni, S., Pasricha, P. J., Lee, G.,

Pomper, M. G., Dawson, V. L., Dawson, T. M., & Ko, H. S. (2019). Transneuronal Propagation of Pathologic α-Synuclein from the Gut to the Brain Models Parkinson's Disease. *Neuron*, *103*(4), 627-641.e7. https://doi.org/10.1016/j.neuron.2019.05.035

[22] Kirkley, K. S., Popichak, K. A., Hammond, S. L., Davies, C., Hunt, L., & Tjalkens, R. B. (2019). Genetic suppression of IKK2/NF-κB in astrocytes inhibits neuroinflammation and reduces neuronal loss in the MPTP-Probenecid model of Parkinson's disease. *Neurobiology of Disease*, *127*, 193–209. https://doi.org/10.1016/j.nbd.2019.02.020

[23] Kwakye, G., Paoliello, M., Mukhopadhyay, S., Bowman, A., & Aschner, M. (2015). Manganese- Induced Parkinsonism and Parkinson's Disease: Shared and Distinguishable Features. *International Journal of Environmental Research and Public Health*, *12*(7), 7519–7540. https://doi.org/10.3390/ijerph120707519

[24] Liddelow, S. A., Guttenplan, K. A., Clarke, L. E., Bennett, F. C., Bohlen, C. J., Schirmer, L., Bennett, M. L., Münch, A. E., Chung, W.-S., Peterson, T. C., Wilton, D. K., Frouin, A., Napier, B. A., Panicker, N., Kumar, M., Buckwalter, M. S., Rowitch, D. H., Dawson, V. L., Dawson, T. M., … Barres, B. A. (2017a). Neurotoxic reactive astrocytes are induced by activated microglia. *Nature*, *541*(7638), 481–487. https://doi.org/10.1038/nature21029

[25] Liu, C., Voth, D. W., Rodina, P., Shauf, L. R., & Gonzalez, G. (1970). A Comparative Study of the Pathogenesis of Western Equine and Eastern Equine Encephalomyelitis Viral Infections in Mice by Intracerebral and Subcutaneous Inoculations. *The Journal of Infectious Diseases*, *122*(1–2), 53–63. https://doi.org/10.1093/infdis/122.1-2.53

[26] Liu, Y., Liu, X., Hao, W., Decker, Y., Schomburg, R., Fulop, L., Pasparakis, M., Menger, M. D., & Fassbender, K. (2014). IKK Deficiency in Myeloid Cells Ameliorates Alzheimer's Disease- Related Symptoms and Pathology. *Journal of Neuroscience*, *34*(39), 12982–12999. https://doi.org/10.1523/JNEUROSCI.1348-14.2014

[27] Maiti, P., Manna, J., & Dunbar, G. L. (2017). Current understanding of the molecular mechanisms in Parkinson's disease: Targets for potential treatments. *Translational Neurodegeneration*, *6*(1), 28. https://doi.org/10.1186/s40035-017-0099-z

[28] Matejuk, A., & Ransohoff, R. M. (2020). Crosstalk Between Astrocytes and Microglia: An Overview. *Frontiers in Immunology*, *11*, 1416. https://doi.org/10.3389/fimmu.2020.01416

[29] Mizuno, Y., Hattori, N., Mori, H., Suzuki, T., & Tanaka, K. (2001). Parkin and Parkinson's disease: *Current Opinion in Neurology*, *14*(4), 477–482. https://doi.org/10.1097/00019052-200108000-00008

[30] Morais, V. A., Verstreken, P., Roethig, A., Smet, J., Snellinx, A., Vanbrabant, M., Haddad, D., Frezza, C., Mandemakers, W., Vogt-Weisenhorn, D., Van Coster, R., Wurst, W., Scorrano, L.,& De Strooper, B. (2009). Parkinson's disease mutations in PINK1 result in decreased Complex I activity and deficient synaptic function. *EMBO Molecular Medicine*, *1*(2), 99–111. https://doi.org/10.1002/emmm.200900006

[31] Moreno, J. A., Yeomans, E. C., Streifel, K. M., Brattin, B. L., Taylor, R. J., & Tjalkens, R. B. (2009). Age-Dependent Susceptibility to Manganese-Induced Neurological Dysfunction. *Toxicological Sciences*, *112*(2), 394–404. https://doi.org/10.1093/toxsci/kfp220

[32] Mosharov, E. V., & Sulzer, D. (2009). Convergence of multiple hits that could underlie Parkinson's disease. *Future Neurology*, *4*(5), 525–529. https://doi.org/10.2217/fnl.09.40

[33] Nandipati, S., & Litvan, I. (2016). Environmental Exposures and Parkinson's Disease.

International Journal of Environmental Research and Public Health, *13*(9), 881. https://doi.org/10.3390/ijerph13090881

[34] Marras, C., Beck, J. C., Bower, J. H., Roberts, E., Ritz, B., Ross, G. W., Abbott, R. D., Savica, R., Van Den Eeden, S. K., Willis, A. W., & Tanner, C. (2018). Prevalence of Parkinson's disease across North America. *Npj Parkinson's Disease*, *4*(1), 21. https://doi.org/10.1038/s41531-018-0058-0

[35] Phillips, A. T., Stauft, C. B., Aboellail, T. A., Toth, A. M., Jarvis, D. L., Powers, A. M., & Olson, K. E. (2013). Bioluminescent Imaging and Histopathologic Characterization of WEEV Neuroinvasion in Outbred CD-1 Mice. *PLoS ONE*, *8*(1), e53462. https://doi.org/10.1371/journal.pone.0053462

[36] Priego, N., & Valiente, M. (2019a). The Potential of Astrocytes as Immune Modulators in Brain Tumors. *Frontiers in Immunology*, *10*, 1314. https://doi.org/10.3389/fimmu.2019.01314

[37] Rey, N. L., Steiner, J. A., Maroof, N., Luk, K. C., Madaj, Z., Trojanowski, J. Q., Lee, V. M.-Y., & Brundin, P. (2016a). Widespread transneuronal propagation of α-synucleinopathy triggered in olfactory bulb mimics prodromal Parkinson's disease. *Journal of Experimental Medicine*, *213*(9), 1759–1778. https://doi.org/10.1084/jem.20160368

[38] Saggu, R., Schumacher, T., Gerich, F., Rakers, C., Tai, K., Delekate, A., & Petzold, G. C. (2016). Astroglial NF-kB contributes to white matter damage and cognitive impairment in a mouse model of vascular dementia. *Acta Neuropathologica Communications*, *4*(1), 76. https://doi.org/10.1186/s40478-016-0350-3

[39] Sarkar, S., Malovic, E., Jin, H., Kanthasamy, A., & Kanthasamy, A. G. (2019). The

role of manganese in neuroinflammation. In *Advances in Neurotoxicology* (Vol. 3, pp. 121–131). Elsevier. https://doi.org/10.1016/bs.ant.2018.10.005

[40] Schultz, D. R., Barthal, J. S., & Garrett, C. (1977). Western equine encephalitis with rapid onset of parkinsonism. *Neurology*, *27*(11), 1095–1095. https://doi.org/10.1212/WNL.27.11.1095

[41] Sofroniew, M. V. (2009a). Molecular dissection of reactive astrogliosis and glial scar formation. *Trends in Neurosciences*, *32*(12), 638–647. https://doi.org/10.1016/j.tins.2009.08.002

[42] Stuart, S. A., & Robinson, E. S. J. (2015). Reducing the stress of drug administration: Implications for the 3Rs. *Scientific Reports*, *5*(1), 14288. https://doi.org/10.1038/srep14288

[43] Sulzer, D. (2007). Multiple hit hypotheses for dopamine neuron loss in Parkinson's disease. *Trends in Neurosciences*, *30*(5), 244–250. https://doi.org/10.1016/j.tins.2007.03.009

[44] Tolosa, E., Vila, M., Klein, C., & Rascol, O. (2020). LRRK2 in Parkinson disease: Challenges of clinical trials. *Nature Reviews Neurology*, *16*(2), 97–107. https://doi.org/10.1038/s41582-019-0301-2

[45] Wendeln, A.-C., Degenhardt, K., Kaurani, L., Gertig, M., Ulas, T., Jain, G., Wagner, J., Häsler, L.M., Wild, K., Skodras, A., Blank, T., Staszewski, O., Datta, M., Centeno, T. P., Capece, V., Islam, Md. R., Kerimoglu, C., Staufenbiel, M., Schultze, J. L., … Neher, J. J. (2018). Innate immune memory in the brain shapes neurological disease hallmarks. *Nature*, *556*(7701), 332– 338. https://doi.org/10.1038/s41586-018-0023-4

[46] Zhou, B., Zuo, Y., & Jiang, R. (2019a). Astrocyte morphology: Diversity, plasticity, and role in neurological diseases. *CNS Neuroscience & Therapeutics*, *25*(6), 665–673.

https://doi.org/10.1111/cns.13123

[47] Spilsbury BH. Discussion on Influenza. *Proc R S Med.* 1919;12:57

[48] Dauer, W., & Przedborski, S. (2003). Parkinson's Disease. *Neuron*, *39*(6), 889–909. https://doi.org/10.1016/S0896-6273(03)00568-3

[49] Stefanis, L. (2012). -Synuclein in Parkinson's Disease. *Cold Spring Harbor Perspectives in Medicine*, *2*(2), a009399–a009399. https://doi.org/10.1101/cshperspect.a009399

[50] Luk, K. C., Song, C., O'Brien, P., Stieber, A., Branch, J. R., Brunden, K. R., Trojanowski, J.Q., & Lee, V. M.-Y. (2009). Exogenous -synuclein fibrils seed the formation of Lewy body-like intracellular inclusions in cultured cells. *Proceedings of the National Academy of Sciences*, *106*(47), 20051–20056. https://doi.org/10.1073/pnas.0908005106

[51] Blandini, F., Nappi, G., Tassorelli, C., & Martignoni, E. (2000). Functional changes of the basal ganglia circuitry in Parkinson's disease. *Progress in Neurobiology*, *62*(1), 63–88. https://doi.org/10.1016/S0301-0082(99)00067-2

[52] Lashuel, H. A., Overk, C. R., Oueslati, A., & Masliah, E. (2013). The many faces of α-synuclein: From structure and toxicity to therapeutic target. *Nature Reviews Neuroscience*, *14*(1), 38–48. https://doi.org/10.1038/nrn3406

[53] Yang, W., Hamilton, J. L., Kopil, C., Beck, J. C., Tanner, C. M., Albin, R. L., Ray Dorsey, E., Dahodwala, N., Cintina, I., Hogan, P., & Thompson, T. (2020). Current and projected future economic burden of Parkinson's disease in the U.S. *Npj Parkinson's Disease*, *6*(1), 15. https://doi.org/10.1038/s41531-020-0117-1

[54] Rizek, P., Kumar, N., & Jog, M. S. (2016). An update on the diagnosis and treatment of Parkinson disease. *Canadian Medical Association Journal*, *188*(16), 1157–1165. https://doi.org/10.1503/cmaj.151179

[55] Jang, H., Boltz, D. A., Webster, R. G., & Smeyne, R. J. (2009). Viral parkinsonism. *Biochimica et Biophysica Acta (BBA) - Molecular Basis of Disease*, *1792*(7), 714–721. https://doi.org/10.1016/j.bbadis.2008.08.001

[56] Ronca, S. E., Dineley, K. T., & Paessler, S. (2016). Neurological Sequelae Resulting from Encephalitic Alphavirus Infection. *Frontiers in Microbiology*, *7*. https://doi.org/10.3389/fmicb.2016.00959

[57] Simon LV, Coffey R, Fischer MA. Western Equine Encephalitis. [Updated 2020 Aug 22]. In: StatPearls [Internet]. Treasure Island (FL): StatPearls Publishing

[58] Al-anbaky, Q., Al-karakooly, Z., Kilaparty, S. P., Agrawal, M., Albkuri, Y. M., RanguMagar, A. B., Ghosh, A., & Ali, N. (2016). Cytotoxicity of Manganese (III) Complex in Human Breast Adenocarcinoma Cell Line Is Mediated by the Generation of Reactive Oxygen Species Followed by Mitochondrial Damage. *International Journal of Toxicology*, *35*(6), 672–682. https://doi.org/10.1177/1091581816659661

[59] Andruska, K. M., & Racette, B. A. (2015). Neuromythology of Manganism. *Current Epidemiology Reports*, *2*(2), 143–148. https://doi.org/10.1007/s40471-015-0040-x

[60] Carriba, P., & Comella, J. (2015). Neurodegeneration and neuroinflammation: Two processes, one target. *Neural Regeneration Research*, *10*(10), 1581. https://doi.org/10.4103/1673-5374.165269

[61] Yang, D., Elner, S. G., Bian, Z.-M., Till, G. O., Petty, H. R., & Elner, V. M. (2007). Pro- inflammatory cytokines increase reactive oxygen species through mitochondria and NADPH oxidase in cultured RPE cells. *Experimental Eye Research*, *85*(4), 462–472. https://doi.org/10.1016/j.exer.2007.06.013

[62] Atik, A., Stewart, T., & Zhang, J. (2016). Alpha-Synuclein as a Biomarker for Parkinson's Disease: Alpha-Synuclein as a Biomarker for PD. *Brain Pathology*, *26*(3), 410–418. https://doi.org/10.1111/bpa.12370

[63] Manzoni, C., Mamais, A., Dihanich, S., Abeti, R., Soutar, M. P. M., Plun-Favreau, H., Giunti, P., Tooze, S. A., Bandopadhyay, R., & Lewis, P. A. (2013). Inhibition of LRRK2 kinase activity stimulates macroautophagy. *Biochimica et Biophysica Acta (BBA) - Molecular Cell Research*, *1833*(12), 2900–2910. https://doi.org/10.1016/j.bbamcr.2013.07.020

[64] Singleton, A. B., Farrer, M. J., & Bonifati, V. (2013). The genetics of Parkinson's disease: Progress and therapeutic implications: The Genetics of PD. *Movement Disorders*, *28*(1), 14–23. https://doi.org/10.1002/mds.25249

[65] Wallings, R., Manzoni, C., & Bandopadhyay, R. (2015). Cellular processes associated with LRRK2 function and dysfunction. *FEBS Journal*, *282*(15), 2806–2826. https://doi.org/10.1111/febs.13305

[66] Jäkel, S., & Dimou, L. (2017). Glial Cells and Their Function in the Adult Brain: A Journey through the History of Their Ablation. *Frontiers in Cellular Neuroscience*, *11*. https://doi.org/10.3389/fncel.2017.00024

[67] Stevenson, R., Samokhina, E., Rossetti, I., Morley, J. W., & Buskila, Y. (2020).

Neuromodulation of Glial Function During Neurodegeneration. *Frontiers in Cellular Neuroscience*, *14*, 278. https://doi.org/10.3389/fncel.2020.00278

[68] Sulzer, D., Antonini, A., Leta, V., Nordvig, A., Smeyne, R. J., Goldman, J. E., Al-Dalahmah, O., Zecca, L., Sette, A., Bubacco, L., Meucci, O., Moro, E., Harms, A. S., Xu, Y., Fahn, S., & Ray Chaudhuri, K. (2020). COVID-19 and possible links with Parkinson's disease and parkinsonism: From bench to bedside. *Npj Parkinson's Disease*, *6*(1), 18. https://doi.org/10.1038/s41531-020-00123-0

[69] Tapias, V., Greenamyre, J. T., & Watkins, S. C. (2013). Automated imaging system for fast quantitation of neurons, cell morphology and neurite morphometry in vivo and in vitro. *Neurobiology of Disease*, *54*, 158–168. https://doi.org/10.1016/j.nbd.2012.11.018